P H Y S I C A L   R E V I E W   L E T T E R S

Generation of Narrow-Bandwidth Paired Photons: Use of a Single Driving Laser

Pavel Kolchin,* Shengwang Du, Chinmay Belthangady, G. Y. Yin, and S. E. Harris

Edward L. Ginzton Laboratory, Stanford University, Stanford, California 94305, USA
(Received 9 June 2006; published 12 September 2006)

We describe a generator of narrow-band paired photons. A single retroreflected Ti:sapphire laser is used to cool, render transparent, and parametrically pump a cloud of ^{87}Rb atoms. We attain a paired-photon generation rate into opposing fibers of 600 counts/s with an intensity correlation function that has a width of 5 ns, and violates the Cauchy-Schwartz criteria by a factor of 2000.

It is an objective of quantum optics [1] to develop generators of time-energy entangled photons with controllable waveforms. A major step was made by the groups of Lukin and Kimble who demonstrated the use of electromagnetically induced transparency (EIT) to generate single photons on demand and to show nonclassical correlations of paired photons [2,3]. More recently, Balić *et al.* [4] at Stanford demonstrated generation and rudimentary waveform shaping of narrow-band biphoton waveforms. Black *et al.* [5] at MIT demonstrated single photon generation on demand with a photon conversion efficiency of 40%.

This Letter describes a modification of the earlier Stanford technique. Its principal features are the use of a standing wave right angle geometry, and the use of a single driving laser with two AOM's to parametrically pump the ^{87}Rb atoms, and also to trap and cool these atoms. This technique results in a modification and narrowing of the Glauber intensity correlation function, and at the same time the elimination of Rayleigh scattering. An energy level diagram, and the geometry and timing for the experiment are shown in Fig. 1. We replace the three driving lasers of the earlier experiment with a single (Ti:sapphire) laser. The Ti:sapphire laser frequency is down-shifted by 123.5 MHz so as to be resonant with the $|5S_{1/2}, F = 2\rangle \rightarrow |5P_{3/2}, F = 2\rangle$ transition. This frequency, denoted by ω_p, acts as the coupling laser of earlier experiments and creates transparency on the $|5S_{1/2}, F = 1\rangle \rightarrow |5P_{3/2}, F = 2\rangle$ transition. This same frequency pumps the four wave downconversion process that generates the paired photons. To cool and trap ^{87}Rb atoms the incident Ti:sapphire laser beam is up-shifted by 123.5 MHz to 20 MHz below the $|5S_{1/2}, F = 2\rangle \rightarrow |5P_{3/2}, F = 3\rangle$ transition (not shown). This is done periodically so as to create a 10% duty cycle, with the trapping process occurring for 4.5 ms, followed by an experimental window of 500 μs. The trapping magnetic field remains on during this experimental window.

Of importance we find that the use of a retroreflected laser for both pumping and coupling results in an unexpected change in the shape of the Glauber intensity correlation function for the Stokes and anti-Stokes photons. In the earlier Stanford work [4], the shape of the correlation function was set by the longer of two characteristic times.

These times are the group delay time between the Stokes and anti-Stokes photons, and the inverse Rabi frequency of the coupling laser. Here, because of the much larger Rabi frequency (200 MHz) of the common pump and coupling laser, the group delay time is short and the Rabi period dominates. We therefore expect a damped-periodic correlation function similar to that of the earlier work with a period of about 5 ns. We find experimentally and verify theoretically that the interference fringes (in the x direction) that are caused by the counterpropagating pumping beams result in a reduction of the outer Rabi side lobes of the intensity correlation function.

We first modify the theory as given by Balic *et al.* [4] and Kolchin [6] to include the periodic variation with x of the pump laser field. We expand Stokes and anti-Stokes field
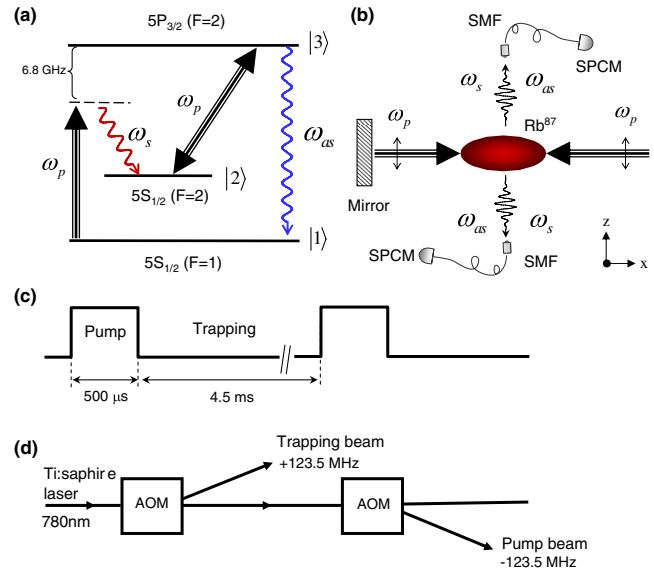

FIG. 1 (color online).   (a) Energy level diagram. (b) Schematic for paired-photon generation. In the presence of a strong, linear polarized, retroreflected pump beam, Stokes and anti-Stokes photons are generated into opposing single mode fibers. The fibers are aligned at right angles to the direction of the pump beam. (c) The photon generation window of 500 μs is followed by a trapping and cooling period of 4.5 ms. (d) The Ti:sapphire laser is up-shifted to trap and cool atoms and down-shifted to serve as a pump for the paired-photon generation process.

113602-1

operators into a sum of spatial modes as $a_S^\dagger(-\omega, z, x) = \sum_{n=-\infty}^{+\infty} a_{S,n}^\dagger(-\omega, z)\exp(ik_n x)$ and $a_{AS}(\omega, z, x) = \sum_{n=-\infty}^{+\infty} a_{AS,n}(\omega, z)\exp(ik_n x)$, where $k_n = 2nk$ with $k = \omega_p/c$. Of these modes, only the zeroth order modes are coupled to the opposing single mode optical fibers. One may show that at the low atom densities of this work, where the medium is reasonably transparent, the interaction of this mode with other modes is negligible. Therefore, the slowly varying amplitude equations for the frequency domain operators $a_{S,0}^\dagger(-\omega, z)$ and $a_{AS,0}(\omega, z)$ are

$$\frac{\partial}{\partial z}a_{S,0}^\dagger + \langle g_R\rangle a_{S,0}^\dagger + \langle\kappa_S\rangle a_{AS,0} = F_{S,0}$$
$$-\frac{\partial}{\partial z}a_{AS,0} + \langle\Gamma_{AS}\rangle a_{AS,0} + \langle\kappa_{AS}\rangle a_{S,0}^\dagger = F_{AS,0}. \quad (1)$$

Here $\langle\cdots\rangle$ denotes the averaging over the period $\Delta x = \lambda/2$ in the x direction, where λ is the pump laser wavelength. For example, $\langle\Gamma_{AS}\rangle = 1/\Delta x \int_0^{\Delta x}\Gamma_{AS}(\omega, x)dx$. $F_{S,0}$ and $F_{AS,0}$ are the commutator preserving Langevin operators for the $n = 0$ mode; $\Gamma_{AS}(\omega, x)$, $g_R(\omega, x)$, $\kappa_S(\omega, x)$, and $\kappa_{AS}(\omega, x)$ are the EIT profile, Raman gain, and parametric coupling coefficients.

With the assumption that the atomic population remains in the ground state,

$$\Gamma_{As} = -\frac{2iN\sigma\gamma_{13}(\omega + i\gamma_{12})}{D(\omega)},$$
$$g_R = \left(\frac{\Omega_p^2}{2\Delta\omega_{13}^2}\right)\frac{iN\sigma\gamma_{13}(\omega + \Delta\omega_{23} + i\gamma_{13})}{D(\omega)}, \quad (2)$$
$$\kappa_S = -\kappa_{AS} = \left(\frac{\Omega_p}{2\Delta\omega_{13}}\right)\frac{iN\sigma\gamma_{13}\Omega_c}{D(\omega)},$$

where $D(\omega) = |\Omega_c|^2 - 4(\omega + i\gamma_{12})(\omega + \Delta\omega_{23} + i\gamma_{13})$. Because of the standing wave, Ω_c and Ω_p are periodic function of x with a period of $2\pi/k$, that is $\Omega_c = \Omega_{c0}\sin(kx)$ and $\Omega_p = \Omega_{p0}\sin(kx)$. The quantities $\Delta\omega_{13}$ and $\Delta\omega_{23}$ are the detunings of the pump laser from the $|1\rangle \to |3\rangle$ and the $|2\rangle \to |3\rangle$ transitions; Ω_p and Ω_c are their Rabi frequencies, and γ_{12} and γ_{13} are their dephasing rates. N is the atom density and σ is the absorption cross section of all allowed transitions.

Figure 2 shows the modification of the anti-Stokes transmission profile and the intensity correlation function that results from the averaged quantities as described above. The parameters for these curves are $N\sigma L = 7.3$ and $\gamma_{12} = 0.6\gamma_{13}$. The pump is tuned to resonance with the $|2\rangle \to |3\rangle$ transition. As seen from Fig. 2(a) the anti-Stokes transition is no longer transparent. The theoretical value of the transmission drops from 99.7% to about 80% at the center of the line. This prediction agrees well with the experimentally measured transmission of 75% ± 10%. The paired-photon rate for each curve is equal to the area under the intensity correlation curve minus the area under the uncorrelated flat background. The changes in the correlation function,

shown in Fig. 2(b), result in the decrease of the paired-photon rate by a factor of ~6.

Paired-photon generation is achieved in an atomic cloud ≈1 mm in diameter that contains about 10^8 atoms at an estimated temperature of 100 μK. The optical depth on the opaque $|1\rangle \to |3\rangle$ transition is 7.3. The pump laser beam has a power of 160 mW and a linewidth of about 1 MHz. It is collimated to a diameter of 1.6 mm and completely overlaps the atomic cloud. In order to detect the photons that are generated into the single mode fibers, we use Perkin-Elmer SPCM-AQR-13 photon counting modules. A time-to-digital converter (Fast Comtec TDC 7888) measures the time between each "start" photon and "stop" photon. Correlation statistics are binned into 512-bin histograms with a bin width of 1 ns. Because of the polarization of the pump beam Rayleigh scatter is eliminated in the z direction. The elimination of Rayleigh scatter reduces the uncorrelated background noise and no additional optical filters are necessary to observe the biphoton intensity correlation function.

The principal results of this work are shown in Fig. 3 and 4. In both figures we plot coincidence counts versus delay time between the Stokes and anti-Stokes photons. In Fig. 3, the pump laser is tuned to resonance of the $|2\rangle \to |3\rangle$ transition. In Fig. 4 the pump is tuned 73 MHz from resonance. Since Stokes and anti-Stokes photons are present in both fibers, the correlation function is symmetric.

As seen from Fig. 3(a) and 3(b), the correlation time may be varied by changing the Rabi frequency of the pumping laser Ω_c. For example, with a pump power of 160 mW focused to an area of 0.02 cm², the calculated (RMS) value of the Rabi frequency $\Omega_c = 170$ MHz and the observed (FWHM) width of the intensity correlation function is 4 ns. When the pump is tuned by $\Delta\omega = 73$ MHz from the resonance as in Fig. 4, we find that the observed oscillation period fits the functional form $1/\sqrt{\Omega_c^2 + \Delta\omega^2}$.
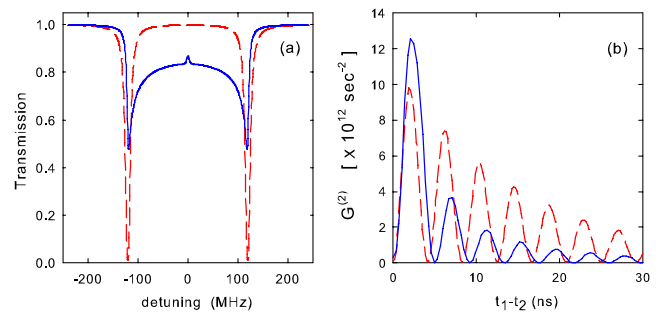

FIG. 2 (color online). (a) Anti-Stokes transmission vs the detuning from the $|1\rangle \to |3\rangle$ transition in the presence of the pump (coupling) laser, (b) non-normalized intensity correlation function $G^{(2)}(t_1 - t_2)$. The transmission and $G^{(2)}(t_1 - t_2)$ are calculated for two cases: (1) there is no interference; $\Omega_c = 80\gamma_{13}$ and $\Omega_p = 140\gamma_{13}$ (dashed curves). (2) There is interference; $\Omega_{c0} = 80\gamma_{13}$ and $\Omega_{p0} = 140\gamma_{13}$ (solid curves).
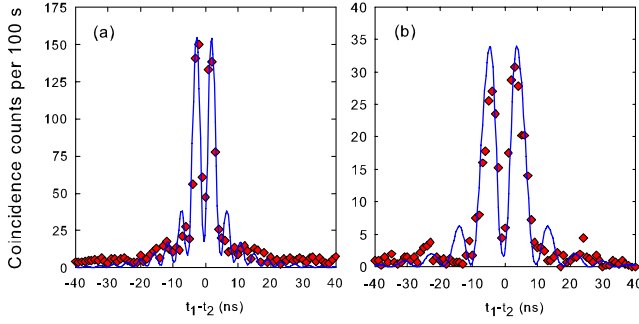
FIG. 3 (color online). Coincidence count rate as a function of the delay between detected photons. (a) Pump power = 160 mW; $\Omega_{c0} = 80\gamma_{13}$ and $\Omega_{p0} = 140\gamma_{13}$. (b) Pump power = 40 mW; $\Omega_{c0} = 40\gamma_{13}$ and $\Omega_{p0} = 70\gamma_{13}$. The pump is tuned to resonance with the $|2\rangle \rightarrow |3\rangle$ transition. Data ($\diamondsuit$) were collected over 200 s. Theoretical curves (solid lines) are scaled vertically by a common factor and are averaged over a 1 ns bin.

At a pump power of 160 mW we observe a paired-photon generation rate of ≈ 12 photons per second. Taking into account the efficiency of each photodetector of 50%, a duty cycle of 10% and the fiber coupling efficiency of 80%, this corresponds to a generation rate of 600 paired photons per second. At this same pump power, we observe ≈ 2200 uncorrelated counts per second in each fiber. Scaling for the efficiency of a single detector and the 10% duty cycle this corresponds to 4.4×10^4 photons $\times$ sec^{-1}. Therefore, the ratio of paired counts to uncorrelated counts is 1.4%.

We compare the experimental results and the theoretical predictions. As seen from Fig. 3 and 4 the shapes of the experimental and theoretical intensity correlation functions are in reasonable agreement. We obtain the theoretical curves (solid lines) by numerically solving Eq. (1) and then evaluating and symmetrizing the intensity correlation function. The pump Rabi frequency, that we use in calcu-
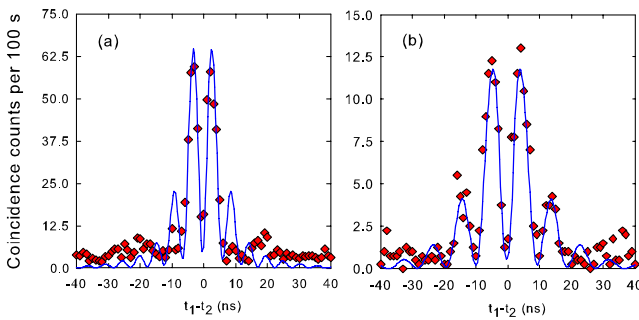

FIG. 4 (color online). Coincidence count rate as a function of the delay between detected photons. (a) Pump power = 80 mW; $\Omega_{c0} = 56\gamma_{13}$ and $\Omega_{p0} = 100\gamma_{13}$. (b) Pump power = 20 mW; $\Omega_{c0} = 28\gamma_{13}$ and $\Omega_{p0} = 50\gamma_{13}$. The pump is tuned 73 MHz above the $|2\rangle \rightarrow |3\rangle$ transition. Data ($\diamondsuit$) were collected over 400 s. Theoretical curves (solid lines) are scaled vertically and are averaged over a 1 ns bin.

lations, is obtained by taking into account the hyperfine structure of the $|5P_{3/2}\rangle$ level. In Fig. 3 and 4(a) the theoretical curves are scaled vertically by a common factor that equals the product of the photodetector efficiencies, the duty cycle, the fiber coupling efficiency, and the inverse of the experiment-theory discrepancy of 14. As estimated above, at a pump power of 160 mW, we achieve a generation rate of 600 paired photons per second, which is lower than the theoretically predicted value by the same discrepancy factor of 14. For Fig. 4(b) the experiment-theory discrepancy is 11.

One measure of performance of a paired-photon light source is the extent to which it violates the Cauchy-Schwartz inequality $[g_{12}^{(2)}(\tau)]^2 \leq g_{11}^{(2)}(0)g_{22}^{(2)}(0)$. In Fig. 3(b), the peak value of the intensity correlation function normalized to uncorrelated background counts is $g_{12}^{(2)} \approx 45$. Using a fiber beam splitter we also measure the peak values of the normalized autocorrelation functions $g_{11}^{(2)} = g_{22}^{(2)} = 1 \pm 0.1$. We obtain a violation of the Cauchy-Schwartz inequality of a factor of ~ 2000. By reducing the pump power we can achieve a higher violation of the Cauchy-Schwartz inequality at the expense of a decrease in the paired-photon rate.

Some years ago [7–10] it was shown that room temperature two-state atoms could be used to produce correlated photons. As a measure of the utility of the present three state source, we measure the correlation function for the two-state system using the cold trapped ^{87}Rb atoms. We use the backward-wave 2° off axis configuration of Balić where correlated photons are generated into opposing directions (Fig. 5). For the two-state transition we use $|5S_{1/2}, F = 2\rangle \rightarrow |5P_{3/2}, F = 3\rangle$ of ^{87}Rb. In order to prepare the atomic population in the ground state the repumping laser remains on. In this experiment the pump laser is tuned above resonance in the range 20 MHz to 100 MHz.

In Fig. 6 we show the intensity correlation function for a pump detuning of 83 MHz. The shape of this intensity correlation function matches well with the theoretical prediction given in Ref. [10]. For the pump detuning of
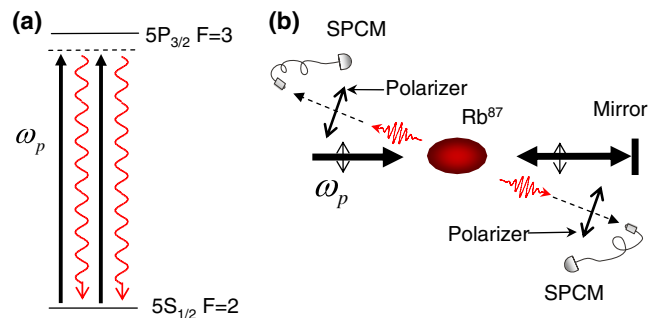

FIG. 5 (color online). (a) Energy level diagram and (b) schematic of the experiment for paired-photon generation in a two-state system. Paired photons are collected at 2° from the direction of the pump beam.
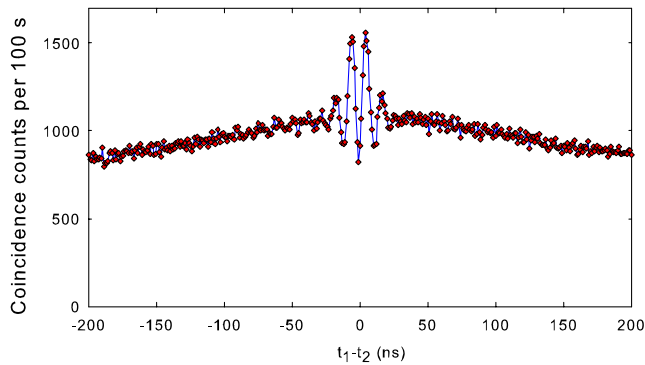
FIG. 6 (color online). Coincidence count rate as a function of the delay between detected photons for paired-photon generation in a two-state system. The experimental data points ($\diamond$) are connected by straight lines. The data are taken with a pump power of 770 μW, a detuning of 83 MHz, and a run time of 200 s.

83 MHz and a power of 770 μW the observed coincidence count rate is about a factor of 10 higher than for the three state system. But the usefulness of the two-state source is diminished by the presence of strong Rayleigh scatter of the pump. Since the uncorrelated count rate (background level) is proportional to the square of the Rayleigh count rate, and therefore to the square of the pump power, the ratio of the peak correlation to background is independent of pump power. For a variety of pump powers and detunings we find that the Cauchy criteria is not violated.

In summary, this Letter has described two types of generators of correlated narrow-band photons. Both types of generators require only a single retroreflected pump laser. The three state source gives the largest violation of the Cauchy criteria thus far reported for narrow-band paired-photon sources [11]. The two-state source has a higher paired count rate, but unless the Rayleigh scatter is filtered out, it has a significantly poorer count to background ratio.

*Electronic address: pkolchin@stanford.edu

[1] D. Bouwmeester, A. Ekert, and A. Zeilinger, *The Physics of Quantum Information* (Springer-Verlag, Berlin, 2000).

[2] C. H. van der Wal, M. D. Eisaman, A. André, R. L. Walsworth, D. F. Phillips, A. S. Zibrov, and M. D. Lukin, Science **301**, 196 (2003).

[3] A. Kuzmich, W. P. Bowen, A. D. Boozer, A. Boca, C. W. Chou, L.-M. Duan, and H. J. Kimble, Nature (London) **423**, 731 (2003).

[4] V. Balić, D. A. Braje, P. Kolchin, G. Y. Yin, and S. E. Harris, Phys. Rev. Lett. **94**, 183601 (2005).

[5] A. T. Black, J. K. Thompson, and V. Vuletić, Phys. Rev. Lett. **95**, 133601 (2005).

[6] P. Kolchin, Phys. Rev. A (to be published).

[7] P. Grangier, G. Roger, A. Aspect, A. Heidmann, and S. Reynaud, Phys. Rev. Lett. **57**, 687 (1986).

[8] A. Heidmann and S. Reynaud, J. Mod. Opt. **34**, 923 (1987).

[9] A. Aspect, G. Roger, S. Reynaud, J. Dalibard, and C. Cohen-Tannoudji, Phys. Rev. Lett. **45**, 617 (1980).

[10] M. W. Mitchell, C. I. Hancox, and R. Y. Chiao, Phys. Rev. A **62**, 043819 (2000).

[11] Recently we became aware that a comparable or stronger violation of the Cauchy criteria has been achieved: J. K. Thompson *et al.*, Science **313**, 74 (2006); J. Laurat *et al.*, quantph/0605122.